Influence of the Silica-to-Surfactant Ratio and the pH of Synthesis on the Characteristics of Mesoporous SBA-15

Ahmad Zuhairi Abdullah*, Noraini Razali and Keat Teong Lee

School of Chemical Engineering, Universiti Sains Malaysia,
Engineering Campus, Seri Ampangan, 14300 USM, Nibong Tebal,
Pulau Pinang, Malaysia

*Corresponding author: chzuhairi@eng.usm.my

Abstract: *Mesoporous silica SBA-15 was synthesised with two different sets of synthesis conditions and was characterised using nitrogen adsorption, X-ray diffraction (XRD), transmission electron microscopy (TEM) and scanning electron microscopy (SEM). The effects of the ratio of tetraethylorthosilicate/triblockcopolymer (TEOS/TCP) (1.52–3.38) and pH (1.3–3.0) were particularly studied. Well-ordered hexagonal mesoporous silicas were formed at a TEOS/TCP ratio of 2.25 and a pH above 2. The highest surface area and an intense XRD pattern were shown by those synthesised at a ratio of 1.52 (669 m^2/g and 0.5 cc/g). A high TEOS amount disturbed the condensation of the silica network, causing failure in the formation of the Si-O-Si network.*

Keywords: mesoporous, SBA-15, TEOS/TCP ratio, pH, characteristics

Abstrak: *Silika mesoliang SBA-15 telah dihasilkan melalui dua set keadaan sintesis yang berbeza dan dicirikan menggunakan kaedah penjerapan nitrogen, pembelauan sinar X (XRD), mikroskop elektron transmisi (TEM) dan mikroskop electron imbasan (SEM). Kesan nisbah tetraetilortosilikat/kopolimer triblok (TEOS/TCP) (1.52–3.38) dan pH (1.3–3.0) telah dikaji secara khusus. Silika heksagon mesoliang yang teratur telah terbentuk pada nisbah TEOS/TCP 2.25 dan pH melebihi 2. Luas permukaan tertinggi dan pola XRD paling kuat ditunjukkan oleh silica yang disintesis pada nisbah 1.52 (669 m^2/g dan 0.5 cc/g). Amaun TEOS yang terlampau tinggi mengganggu kondensasi jaringan silika menyebabkan kegagalan dalam pembentukan jaringan Si-O-Si.*

Katakunci: mesoliang, SBA-15, nisbah TEOS/TCP, pH, ciri-ciri

1. INTRODUCTION

The presence of ordered nanoporous materials has been known for more than a century.[1] Since the discovery of M41S mesoporous materials in 1992, there has been an increasing interest in the design of novel porous materials tailored with various pore organisations and dimensions for potential applications in separation, catalysis, chemical sensing and optical coating.[2,3] The use of mesoporous materials of MCM-41 as carriers for basic guest species has been

proposed by Weitkamp *et al.*[4] This material is usually synthesised in a basic medium and in the presence of surfactant cations.[5] However, MCM-41 material is limited to a pore size of about 80 Å, and, because of this, it is not suitable for processing large biomolecules such as protein and enzymes.[6] Even though this material has a quite high thermal stability, it loses its structure when exposed to high-temperature steam or boiling water. The collapse of the structure limits the applications of MCM-41, especially in catalytic reactions involving aqueous solutions.[7]

Recently, a new type of ordered mesoporous material has attracted great attention in the field of catalysis. SBA-15 materials possess high surface areas (600–1,000 m^2g^{-1}) and are made up of hexagonal arrays of uniform tubular channels with tunable pore diameters in the range of 5–30 nm. The pore walls are thicker (3–6 nm) to provide high thermal stability, so these materials therefore promise great opportunity for application as catalysts and catalytic supports.[8] Because of the variety of practical uses, the fabrication of the desired morphologies of mesoporous silica is as important as the control of its internal structure and porosity. SBA-15 can be readily synthesised using cheap and commercially available organic templating agents (surfactants). The two stages involved in the preparation of SBA-15 are hydrolysis-condensation and the aging stage.[9,10] However, only a few articles addressing morphological controls of SBA-15-type mesoporous silica are available in the literature.[10,11] It is reported that the ratio of the silica source to the surfactant ratio and the pH of the synthesis gel can greatly influence the characteristics of the resulting materials as they generally control the formation of micelles during the synthesis.[8] Hence, many aspects of the synthesis processes are involved in developing these porous materials, and they still require greater insight and understanding.

A basic understanding of the synthesis conditions is indispensable, as mesoporous materials with desirable characteristics can only be obtained by suitably controlled synthesis procedures and conditions.[12] Many studies have indicated that several factors (e.g., temperature, inorganic salt, pH and acid species) could affect the interaction between organic micelles and inorganic species and consequently influence the final structure of the mesoporous materials during the self-assembly process.[13] Variations in the hydrolysis rate of tetraethylorthosilicate (TEOS) and the condensation rate of the silica precursor as a function of pH value have been reported to play significant roles in the formation of high quality mesoporous materials.[13,14] Based on this reasoning, it should be possible to obtain a mesoporous silica with the desired morphology by controlling the hydrolysis and condensation rates of the silica precursor. For that reason, the TEOS to triblockcopolymer (TCP) ratio and the pH effect were chosen to be further investigated in this study. Elucidation of the characteristics of the materials was made based on nitrogen adsorption, X-ray diffraction

(XRD), transmission electron microscopy (TEM) and scanning electron microscopy (SEM) results.

2. EXPERIMENTAL

2.1 Synthesis of SBA-15

The hexagonal mesoporous material (SBA-15) was synthesised using a Pluronic P123 TCP surfactant (EO_{20}-PO_{70}-EO_{20}, Sigma Aldrich, USA; M_{av} = 5800) as the structure directing agent and TEOS (Merck, USA) as the silica source. The surfactant was first dissolved in a 2 M HCl solution at room temperature for 1 h. Then, the silica source was added into this solution under stirring at 40^{o}C for another 2 h, and a precipitated product appeared. The mixture solution with the precipitated product was shaken in a water bath shaker at 40^{o}C with 120 rpm for one day. The precipitated product was then filtered, washed with water and air-dried at room temperature. Finally, calcination was carried out at 500^{o}C for 6 h to remove the organic template. A series of samples were prepared by changing the molar ratio of TEOS/TCP and the pH. The samples were denoted as S1, S2, S3 and S4 for the TEOS/TCP ratios of 1.52, 2.25, 3.15 and 3.38, respectively, while the pH was maintained at 1.7. For the effect of pH, the samples were denoted as S5, S6, S7 and S8 for pH values of 1.3, 1.7, 2.5 and 3.0, respectively, while the TEOS/TCP ratio was maintained at 2.25.

2.2 Characterisation of SBA-15

Nitrogen adsorption/desorption measurements were carried out using a Micromeritic ASAP 2000 (USA) system, and about 0.08 g of sample was used in every test. Prior to the nitrogen adsorption, all samples were degassed at 300^{o}C for 3 h. The data obtained for specific surface area (S_{BET}) were calculated using the Brunauer-Emmett-Teller (BET) method, and total pore volume (V_p) was determined using the single point method at 0.98. Micropore area was calculated using the *t*-plot method. Pore size distribution (PSD) curves were calculated using the Barrett-Joyner-Halenda (BJH) method on the adsorption branch. The position of the maximum point of the PSD was used as the estimated average pore diameter. The nitrogen adsorption-desorption isotherm result was analysed and examined using the physisorption isotherms and hysteresis loops classified by IUPAC as a reference.[15] The crystallisation phases of the synthesised catalyst were studied using the XRD method. The analysis was carried out using a Siemens D5000 (Germany) system operating at 40 kW. The morphology of the mesoporous materials (TEM images) was evaluated using a Philips CM 12 (Netherlands) transmission electron microscope operating at 80 kV. The sample of about 0.05 g was first dissolved in 3 ml of 100% acetone. Then, the solution

was shaken for a few seconds, and the precipitated powder (light powder) was slowly sucked out with a micropipette and dropped on the grid for the analysis. TEM images were recorded at a magnification of 35000 x. SEM was performed using a Leo Supra scanning electron microscope (model 35 VP, Germany). Using a Sputter Coater Polaron SC515 (Quorum Technologies, UK), the samples were first coated with gold (20–30 nm thickness) for better electron reflection.

3. RESULTS AND DISCUSSION

The nitrogen adsorption isotherms of SBA-15 materials synthesised at different ratios of TEOS/TCP are shown in Figure 1, and their corresponding pore size distributions are shown in Figure 2. The isotherms show a sharp step with a hysteresis loop corresponding to the filling of ordered mesopores. For the SBA-15 samples with a TEOS/TCP ratio of 1.52, the isotherm exhibits a large hysteresis loop of type E with a sloping adsorption branch and a steep desorption branch. However, the pore size distributions are broader when higher TEOS/TCP ratios were used. The broader pore size distributions were mainly attributed to lower structural ordering.

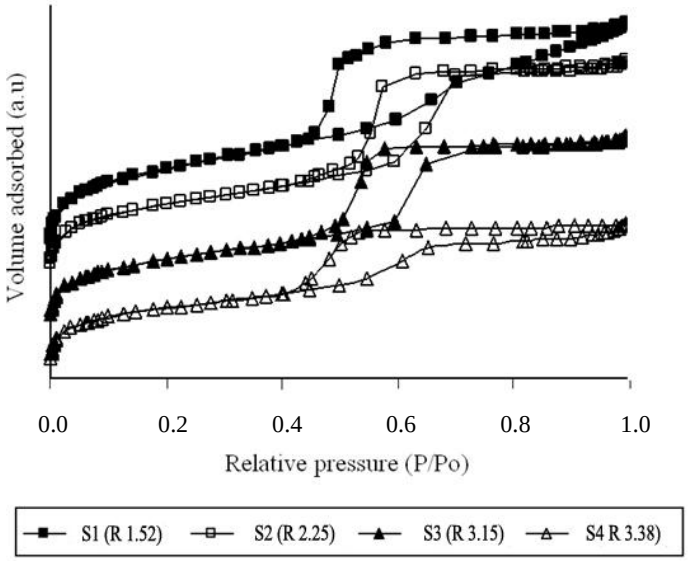

Figure 1: Effects of TEOS/TCP ratio on the nitrogen adsorption-desorption isotherms.
Note: R denotes ratio

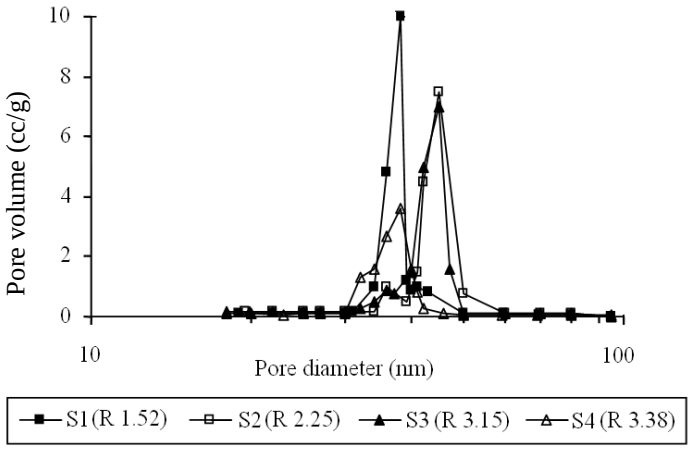

Figure 2: Effects of TEOS/TCP ratio on the pore size distribution.
Note: R denotes ratio

With increasing TEOS content, the surface area, pore volume and pore diameter gradually decreased. The decrease in these properties could be further observed from the data given in Table 1. The samples were synthesised by varying the TEOS/TCP ratio but maintaining the pH value at 1.7. In each sample, the presence of micropores and mesopores was observed. The total micropore area was lower than that of mesopores, indicating that the structure related to mesopores was dominant. The highest surface area and pore volume were shown for the SBA-15 samples synthesised at a TEOS/TCP ratio of 1.52 (S1). About 66.3% of the surface area of this sample was contributed by mesopores, while this value was just 52.0% for the SBA-15 sample with a TEOS/TCP ratio of 3.38 (S4). The considerable decrease in the surface area and pore volume could indicate the failure of Si-O-Si network formation due to the excessive TEOS amount interrupting the condensation of the silica network on the micelles. Thus, the TEOS also affected the siloxane network structure in the pore walls and thereby resulted in changes in microporosity.[11] The systematic change in the microporosity and pore wall thickness of the mesoporous materials indicates the existence of micropores within the mesopore wall. The increase in microporosity was due to the increase of the pore wall thickness.[16]

Table 1: Physical properties for the SBA-15 samples prepared under different conditions.

Sample	Surface area (m^2/g)	Micropore area (m^2/g)	Mesopore area (m^2/g)	Pore diameter (nm)	Pore volume (cc/g)
S1 (R 1.52)	669	225	444	4.95	0.5
S2 (R 2.25)	536	214	322	4.86	0.42
S3 (R 3.15)	520	205	315	4.57	0.42
S4 (R 3.38)	510	246	264	4.35	0.35
S5 (pH 1.3)	679	224	455	3.64	0.38
S6 (pH 1.7)	646	268	378	4.15	0.49
S7 (pH 2.5)	530	223	307	4.74	0.58
S8 (pH 3.0)	488	262	226	4.88	0.59

Note: R denotes ratio

In this study, only pH values in the range of 1.3 to 3.0 were investigated, for which TEOS/TCP was maintained at 2.25. This was in accordance with the specific objective to study the effect of pH in the region that is slightly lower and slightly higher than the isoelectric point of silica. The isoelectric point of silica is at pH 2.[17,18] At this pH, silicic oligomeric species present in gel are positively charged and/or neutral.[13] The results obtained from the nitrogen adsorption-desorption analysis, as shown in Figure 3, reveal that the surface area decreased while the pore diameter and pore volume increased with increasing pH. This phenomenon can be clearly explained based on the understanding of the interactions between the surfactant and silicate. Below a pH of 2.0, the silicate carries a positive charge, while in an alkaline condition the silicate is negatively charged. In the alkaline route, the interaction between the surfactant and silicates is considered to occur through a stronger S^+I^- type electrostatic interaction, where I^- stands for Si-O groups. A higher degree of silicate condensation is achieved at a higher pH value. The more rapid condensation should have less interference on the micelles and should lead to the formation of hexagonal mesoporous silica with fewer defects. However, it will also lead to a lower surface area and pore volume.[19]

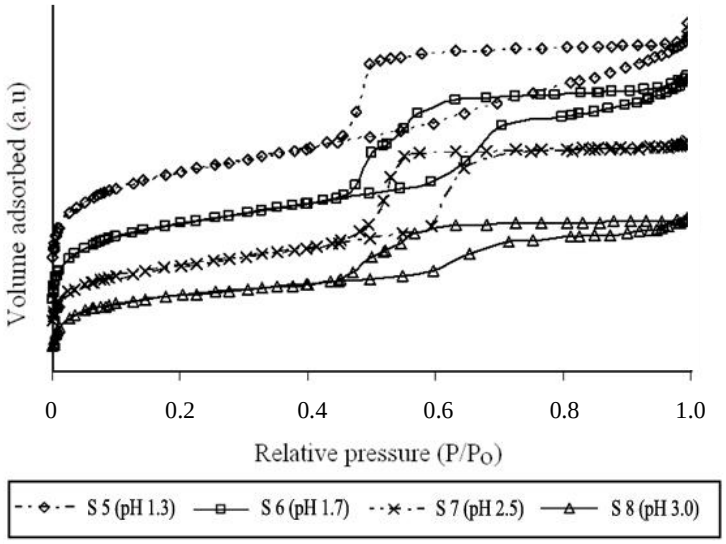

Figure 3: Effects of pH on the nitrogen adsorption-desorption isotherms.

When P123 was mixed with water at or above room temperature, it formed micelles with polypropylene oxide (PPO) cores and hydrated polyethylene oxide (PEO) coronas.[20] The formation of hexagonal mesophase under highly acidic conditions occurred through $S^+H^+X^-I^+$ formation.[21] The protonated silanol groups (Si^-O^+) reacted with positively charged surfactants (S^+) via the counter anions (X^-) through a $S^+X^-I^+$ type electrostatic interaction under highly acidic conditions. Mesoporous silica synthesised in acids was in the form of Si-OH or Si-OH_2^+.[22] The hydrated PEO was protonated or H^+ interacted to the EO part through the electrostatic interaction (S^0H^+) upon the addition of HCl. The hydrophilic region of the surfactant was surrounded by halide ions, forming an electrical double layer.

The role of HCl in the synthesis process involves dehydrating the PEO segment and decreasing the solubility of the PEO block by the presence of Cl^- ions in the aqueous solution.[21] The increase in pore diameter correlates with the fact that the PEO chain becomes dehydrated with increasing amounts of HCl or the presence of large amounts of $C1^-$ ions. Therefore, for the partial dehydration of PEO units, the volume of the hydrophilic part of the micelle decreases. This leads to an increase in the hydrophobic region or hydrophobic domain volume. Subsequently, it leads to an increase in the pore size and a decrease in microporosity.[21] The decreasing microporosity also decreases the surface area.

With the increase in the size of micelles, a corresponding increase in the pore size generally results.[23] It has also been reported by Hung *et al.*[24] that at low pH values, the high concentration of HCl anions would promote the micellisation capability of the TCP, effectively reducing the microporosity of the final product. In this study, it was demonstrated that the mesoporous array was strongly influenced by the pH value. The highest surface areas of silica were observed when the reaction was carried out at lower pH values. Thus, a pH of 1.7 was used for further experiments.

The XRD patterns for the SBA-15 samples synthesised with different TEOS/TCP ratios are shown in Figure 4. In the case of these different silica contents, the XRD patterns show 2 reflections in the 2θ range of 1^{o}–3^{o}. The reflections were due to the ordered hexagonal array of parallel silica tubes and can be indexed as (100) and (200). Since the materials were not crystalline at an atomic level, no reflections at higher angles were observed. When a higher ratio of TEOS/TCP (3.38) was applied, the XRD pattern showed lower intensities for the (100) reflection and did not feature clear (200) reflection. Otherwise, the d(100) spacing and unit cell parameter gradually decreased. The disappearance of these reflections indicates that these samples presented a structural ordering that was lower than that of materials prepared at lower ratios of TEOS/TCP. However, the wall thickness increased with increasing ratio of TEOS/TCP. Sousa and Sousa[25] have suggested that a decrease in wall thickness is associated with an increase in surface area. Therefore, the XRD result was in good agreement with the nitrogen adsorption-desorption results, which suggested that the increasing ratio of TEOS/TCP decreased the surface area but increased the wall thickness.

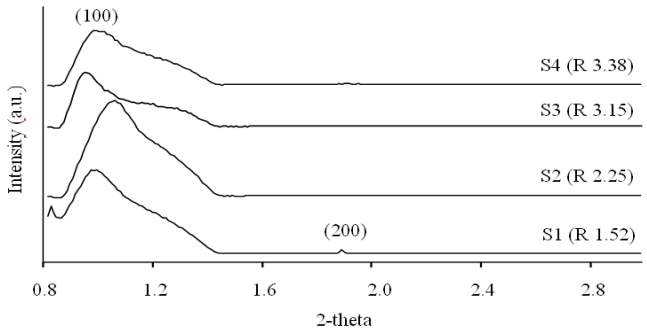

Figure 4: XRD patterns for different mesoporous silicas synthesised at different TEOS/TCP ratios.

Figure 5 shows the XRD patterns for SBA-15 samples synthesised at various pH values and can be indexed as (100) and (200). For pH values lower than 2.0, only one reflection peak (100) appeared. Further increases in the pH value led to the appearance of the second reflection peaks indexed as (200), which were observed when the pH was 2.5 and 3.0. This was attributed to the accelerated hydrolysis of TEOS at lower acid contents, thereby favouring subsequent condensation to form mesopores. The XRD results revealed that with increasing pH, the d(100) spacing and unit cell parameter gradually decreased, as tabulated in Table 2. At low pH values, the surfactant-silica interactions were so weak that the template effect of the surfactant was not very pronounced, and this resulted in the formation of disordered materials.[13] This observation is also in agreement with the reported result by Muto and Imai[17] showing disordered mesostructures forming at pH 1–2, which is around the reported isoelectric point.

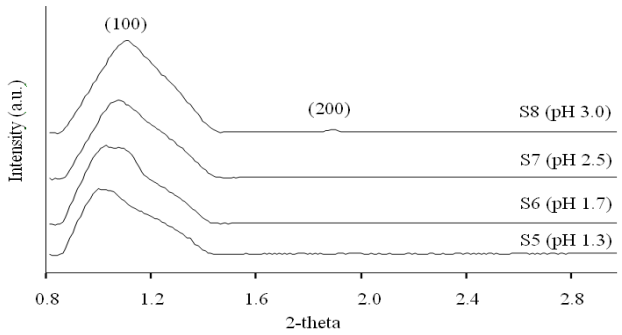

Figure 5: XRD patterns for different mesoporous silicas synthesised at different pH values.

Table 2: Structural parameters from XRD analysis for the SBA-15 samples prepared under different conditions.

Sample	d(100) (nm)	a_o (nm)	Pore diameter, d_{pore} (nm)	Wall thickness, t (nm)
S1 (R 1.52)	8.32	11.54	4.95	6.59
S2 (R 2.25)	8.28	11.48	4.86	6.62
S3 (R 3.15)	8.13	11.27	4.57	6.70
S4 (R 3.38)	8.01	11.11	4.35	6.76
S5 (pH 1.3)	8.69	12.05	3.64	8.41
S6 (pH 1.7)	8.52	11.81	4.15	7.66
S7 (pH 2.5)	7.74	10.73	4.74	5.99
S8 (pH 3.0)	7.24	10.03	4.88	5.15

The influence of the TEOS/TCP ratio on the SBA-15 pore structure is shown in Figure 6. The images indicate that SBA-15 samples synthesised from non-ionic TCPs had high porosities with rather uniform hexagonal arrays of mesopore channels. The TEM images show relatively well-ordered hexagonal mesostructures forming at TEOS/TCP ratios of 1.52 (S1) and 2.25 (S2). However, when the ratio was further increased to 3.38 (S4), the pore wall of the mesoporous structure collapsed at certain areas, giving rise to the disordered mesoporous structure. This was consistent with findings by Calvillo *et al.*[26], who found that disordered mesostructures were formed at a TEOS/P123 ratio of 8.

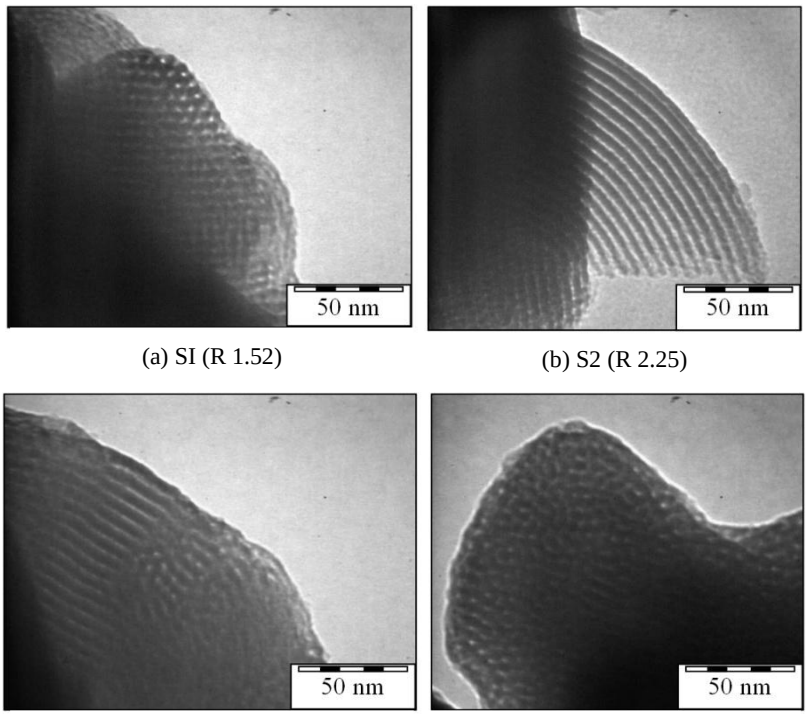

(a) SI (R 1.52) (b) S2 (R 2.25)

(c) S3 (R 3.15) (d) S4 (R 3.38)

Figure 6: TEM images of SBA 15 synthesised at different TEOS/TCP ratios (R) (magnification = 35000 x).

During an inorganic-organic assembling process, the PEO blocks are only accessible to a limited amount of TEOS, and a large quantity of residual TEOS is left behind. Thus, the TEOS/TCP ratio can affect the siloxane network structure.[27] In this study, a large amount of silica precursor (a TEOS/TCP ratio higher than 1.52) caused some amount of the silica precursor to have limited

access to the EO_n blocks of the template (these blocks have been suggested to facilitate the hydrolysis and condensation of TEOS). Consequently, it may not hydrolyse/condense at an accelerated rate. Finally, the excess TEOS could functionalise the silica surface to form irregular silica mesopores.[9]

Figure 7 shows the TEM images of the samples synthesised at different pH values. The differences in morphology were attributed to different interactions between the surfactant and silicate species at different pH values. It is clear from the figure that for the SBA-15 synthesised at a pH of 1.3, undeveloped hexagonal channels were obtained. At pH values below 2.0, the surfactant-silica interactions were so weak that the template effect of the surfactant was not very pronounced, and this resulted in the formation of disordered materials.[13] However, for SBA-15 synthesised at pH values higher than 2.0, the images show well-ordered hexagonal arrays of channels.

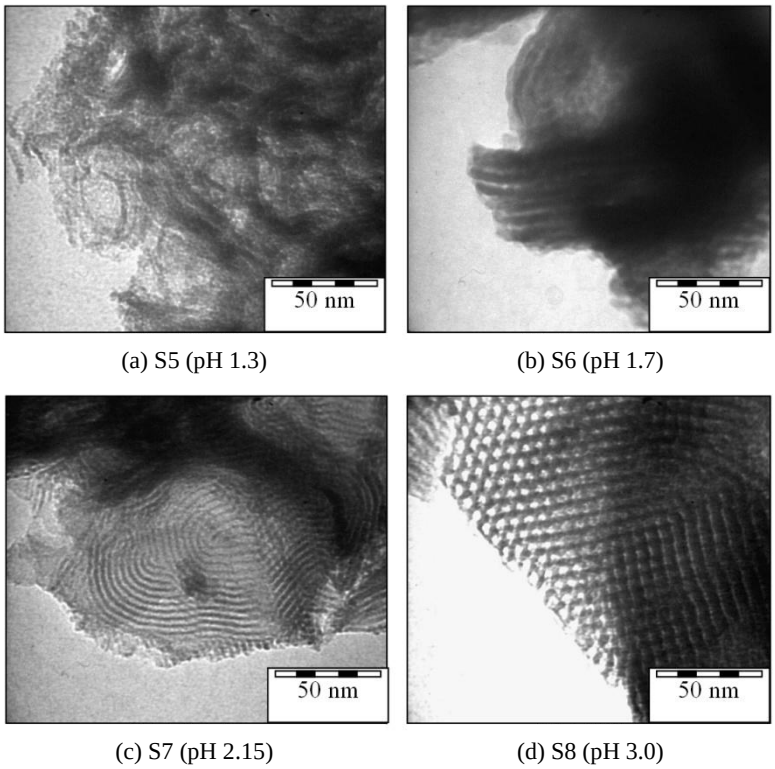

(a) S5 (pH 1.3) (b) S6 (pH 1.7)

(c) S7 (pH 2.15) (d) S8 (pH 3.0)

Figure 7: TEM images of SBA-15 samples synthesised at different pH values (magnification = 35000 x).

The SEM analysis was carried out to specifically examine the topology of the catalyst surfaces and the morphology of the particles and crystals. Figure 8 presents the SEM images of SBA-15 with different TEOS/TCP ratios and pH values. Comparisons between the images of samples with different values for each synthesis variable were made to provide a clearer picture of the specific differences between structures. Again, the results suggest a strong dependence between SBA-15 formation and the synthesis conditions. The images of SBA-15 samples synthesised at a TEOS/TCP ratio of 3.15 showed more cavities compared to those synthesised with a TEOS/TCP ratio of 3.38. This result was attributed to the residual silica precursors that were hydrolysed and preferentially condensed in the copolymer micelles. After surfactant removal through calcination, the condensed amorphous silica deposited on the wall and subsequently covered the pores. For the SEM images of SBA-15 samples synthesised below the isoelectric point (below pH 2.0), fewer cavities were observed. In general, the SEM results for all the synthesis conditions showed good agreement with the results obtained from the nitrogen adsorption-desorption, XRD and TEM analyses.

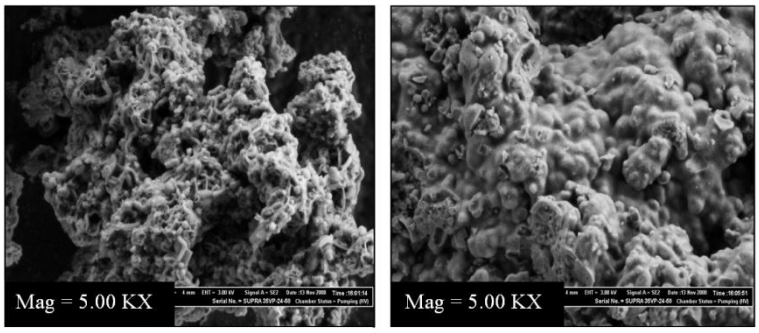

(a) S3 (R 3.15) (b) S4 (R 3.38)

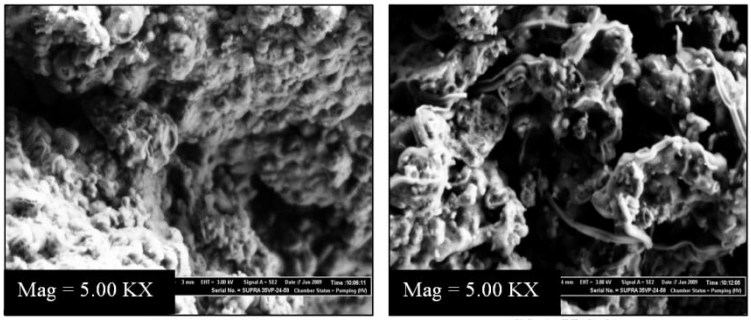

(c) S6 (pH 1.7) (d) S8 (pH 3.0)

Figure 8: SEM images of SBA-15 synthesised under various conditions.

4. CONCLUSION

Highly ordered SBA-15-type mesoporous silica materials were successfully synthesised under different TEOS/TCP ratios and pH values. Their arrays of straight channels were evident under TEM imaging. A well-ordered mesostructure was observed to satisfactorily form at TEOS/TCP ratios lower than 3.15 and pH values above 2.0. The BET surface area was found to decrease and lower intensities of XRD patterns were observed with increasing TEOS/TCP ratio. In addition, the d(100) spacing and unit cell parameter were also found to decrease. The considerable decrease in the surface area and pore volume could indicate the failure of Si-O-Si network formation due to excessive TEOS amounts interrupting the condensation of the silica network on the micelles. Regarding the effect of increasing pH, the BET surface area was found to decrease, but the pore diameter and pore volume showed a reverse trend. The XRD results revealed that the d(100) spacing and unit cell parameter decreased with increasing pH. This phenomenon was clearly explained based on the understanding of the interaction between the surfactant and silicates. Thus, the ratio of TEOS/TCP and the pH were deemed to be important factors in the development of a well-ordered mesoporous material with a high surface area. The optimum conditions for the formation of SBA-15 were obtained, with 1.52 for the TEOS/TCP ratio and a pH of 1.7.

5. ACKNOWLEDGEMENT

The authors gratefully acknowledge the Fundamental Research Grant Scheme (FRGS) from the Ministry of Higher Education, Malaysia, and the Research University (RU) grant from Universiti Sains Malaysia.

6. REFERENCES

1. Meynen, V., Cool, P. & Vansant, E. F. (2007). Synthesis of siliceous materials with micro- and mesoporosity. *Microporous Mesoporous Mater.*, 104, 26–38.
2. Cheng, C. F., Lin, Y. C., Cheng, H. H. & Chen, Y. C. (2003). The effect and model of silica concentrations on physical properties and particle sizes of three-dimensional SBA-16 nanoporous materials. *Chem. Phys. Lett.*, 382(5–6), 496–501.
3. Venkatesan, C., Chidambaram, M. & Singh, A. P. (2005). 3-aminopropyltriethoxysilyl functionalized Na-Al-MCM-41 solid base catalyst for selective preparation of 2-phenylpropionitrile from phenylcetonitrile. *Appl. Catal., A*, 292, 344–353.

4. Weitkamp, J., Hunger, M. & Rymsa, U. (2001). Base catalysis on microporous and mesoporous materials: Recent progress and perspectives. *Microporous Mesoporous Mater.*, 48(1), 255–270.
5. Khodakov, A. Y., Zholobenko, V. L., Bechara, R. & Durand, D. (2005). Impact of aqueous impregnation on the long-range ordering and mesoporous structure of cobalt containing MCM-41 and SBA-15 materials. *Microporous Mesoporous Mater.*, 79(1–3), 29–39.
6. Nguyen, T. P. B., Lee, J. W., Shim, W. G. & Moon, H. (2008). Synthesis of functionalized SBA-15 with ordered large pore size and its adsorption properties of BSA. *Microporous Mesoporous Mater.*, 110(2–3), 560–569.
7. Ooi, Y. S., Zakaria, R., Mohamed, A. R. & Bhatia, S. (2004). Hydrothermal stability and catalytic activity of mesoporous aluminum-containing SBA-15. *Catal. Commun.*, 5(8), 441–445.
8. Berrichi, Z. E., Louis, B., Tessonnier, J. P., Ersen, O., Cherif, L., Ledoux, M. J. & Pham-Huu, C. (2006). One-pot synthesis of Ga-SBA-15: Activity comparison with Ga-post-treated SBA-15 catalysts. *Appl. Catal., A*, 316(2), 219–225.
9. Kruk, M., Jaroneic, M., Joo, S. H. & Ryoo, R. (2003). Characterization of regular and plugged SBA-15 silicas by using adsorption and inverse carbon replication and explanation of the plug formation mechanism. *J. Phys. Chem. B*, 107(10), 2205–2213.
10. Chareonpanich, M., Nanta-ngern, A. & Limtrakul, J. (2007). Short-period synthesis of ordered mesoporous silica SBA-15 using ultrasonic technique. *Mater. Lett.*, 61(29), 5153–5156.
11. Miyazawa, K. & Inagaki, S. (2000). Control of the microporosity within the pore walls of ordered mesoporous silica SBA-15. *Chem. Comm.*, 21, 2121–2122.
12. Fuertes, A. B. (2004). Synthesis of ordered nanoporous carbons of tunable mesopore size by templating SBA-15 silica materials. *Microporous Mesoporous Mater.*, 67(2–3), 273–281.
13. Leonard, A., Blin, J. L., Jacobs, P. A., Grange, P. & Su, B. L. (2003). Chemistry of silica at different concentrations of non-ionic surfactant solutions: Effect of pH of the synthesis gel on the preparation of mesoporous silica. *Microporous Mesoporous Mater.*, 63(1–3), 59–73.
14. Newalkar, B. L. & Komarneni, S. (2001). Control over microporosity of ordered microporous-mesoporous silica SBA-15 framework under microwave-hydrothermal conditions: Effect of salt addition. *Chem. Mater.*, 13(12), 4573–4579.
15. Buchmeiser, M. R. (2003). *Polymeric materials in organic synthesis and catalysis.* Retrieved 11 May 2008 from http://books.google.com.my>.

16. Vradman, L., Titelman, L. & Herskowitz, M. (2006). Size effect on SBA-15 microporosity. *Microporous Mesoporous Mater*., 93(1–3), 313–317.
17. Muto, S. & Imai, H. (2006). Relationship between mesostructures and pH conditions for the formation of silica-cationic surfactant complexes. *Microporous Mesoporous Mater.*, 95(1–3), 200–205.
18. Jin, Z., Wang, X. & Cui, X. (2008). Synthesis and morphological investigation of ordered SBA-15-type mesoporous silica with an amphiphilic triblock copolymer template under various conditions. *Colloids Surf., A*, 316(1–3), 27–36.
19. Liu, M. C., Chang, C. S., Chan, J. C. C., Sheu, H. S. & Cheng, S. (2009). An alkaline route to prepare hydrothermally stable cubic Pm3n mesoporous silica using CTEA template. *Microporous Mesoporous Mater*., 121(1–3), 41–51.
20. Lettow, J. S., Han, Y. J., Schmidt-Winkel, P., Yang, P., Zhao, D., Stucky, G. D. & Ying, J. Y. (2000). Hexagonal to mesocellular foam phase transition in polymer-templated mesoporous silicas. *Langmuir,* 16(22), 8291–8295.
21. Shah, P., Ramaswamy, A. V., Lazar, K. & Ramaswamy, V. (2007). Direct hydrothermal synthesis of mesoporous Sn-SBA-15 materials under weak conditions. *Microporous Mesoporous Mater.*, 100(1–3), 210–226.
22. Mou, C. Y. & Lin, H. P. (2000). Control of morphology in synthesizing mesoporous silica. *Pure Appl. Chem.*, 72(1–2), 137–146.
23. Galarneau, A., Cambon, H., Di Renzo, F., Ryoo, R., Choi, M. & Fajula, F. (2002). Microporosity and connections between pores in SBA-15 mesostructured silicas as a function of the temperature of synthesis. *New J. Chem.*, 27, 73–79.
24. Hung, S. C., Lin, H. P. & Mou, C. Y. (2003). One-step synthesis of mesoporous silica SBA-15 with ultra-high microporosity. *Stud. Surf. Sci. Catal.*, 146, 105–108.
25. Sousa, A. & Sousa, E. M. B. (2006). Influence of synthesis temperature on the structural characteristics of mesoporous silica. *J. Non-Cryst. Solids,* 352(32–35), 3451–3456.
26. Calvillo, L., Celorrio, V., Moliner, R., Cabot, P. L., Esparbe, I. & Lazaro, M. J. (2008). Control of textural properties of ordered mesoporous materials *Microporous Mesoporous Mater.*, 116(1–3), 292–298.
27. Bao, X., Zhao, X. S., Li, X. & Li, J. (2004). Pore structure characterization of large-pore periodic mesoporous organosilicas synthesized with varying SiO_2/template ratios. *Appl. Surf. Sci.*, 237(1–4), 380–386.